Immunology & Cell Biology 2022; **100**: 791–804
www.wileyonlinelibrary.com/journal/icb

ORIGINAL ARTICLE

OPEN

BCL6 deletion in CD4 T cells does not affect Th2 effector mediated immunity in the skin

Jodie Chandler[1], Melanie Prout[1], Sam Old[1], Cynthia Morgan[1], Franca Ronchese[1], Christophe Benoist[2] & Graham Le Gros[1]

1 Malaghan Institute of Medical Research, Wellington, New Zealand
2 Department of Immunology, Harvard Medical School, Boston, MA, USA

Keywords
BCL6, T cell plasticity, Tfh, Th2 differentiation

Correspondence
Graham Le Gros, Malaghan Institute of Medical Research Gate 7, Victoria University, Kelburn Parade, Wellington, New Zealand.
E-mail: glegros@malaghan.org.nz

Received 8 May 2022;
Revised 5 and 20 September 2022;
Accepted 28 September 2022

doi: 10.1111/imcb.12589

Immunology & Cell Biology 2022; **100**: 791–804

Abstract

Recent studies propose that T follicular helper (Tfh) cells possess a high degree of functional plasticity in addition to their well-defined roles in mediating interleukin-4-dependent switching of germinal center B cells to the production of immunoglobulin (Ig)G1 and IgE antibodies. In particular Tfh cells have been proposed to be an essential stage in Th2 effector cell development that are able to contribute to innate type 2 responses. We used CD4-cre targeted deletion of BCL6 to identify the contribution Tfh cells make to tissue Th2 effector responses in models of atopic skin disease and lung immunity to parasites. Ablation of Tfh cells did not impair the development or recruitment of Th2 effector subsets to the skin and did not alter the transcriptional expression profile or functional activities of the resulting tissue resident Th2 effector cells. However, the accumulation of Th2 effector cells in lung Th2 responses was partially affected by BCL6 deficiency. These data indicate that the development of Th2 effector cells does not require a BCL6 dependent step, implying Tfh and Th2 effector populations follow separate developmental trajectories and Tfh cells do not contribute to type 2 responses in the skin.

INTRODUCTION

The cellular and molecular events surrounding the allergen induced differentiation of CD4 T follicular helper (Tfh) cells requires the expression of the transcription factor (TF) BCL6,[1,2] the surface expression of CXCR5 enabling the retention Tfh cells in the germinal centers and the production of the cytokines interleukin (IL)-21 and IL-4 for driving B cell class switching to immunoglobulin (Ig)G1 and IgE.[3–7] Although Tfh cells are classically regarded as a fully differentiated CD4 T cell subset, recent reports indicate that in some experimental models Tfh retain a degree of functional plasticity, are capable of expressing canonical cytokines of all Th lineages and can circulate in the blood and retain the ability to differentiate into effector memory cells.[8] Tfh cells have been shown to differentiate from Th2 committed precursors in the draining lymph node (dLN) after immunization with *Schistosoma mansoni* eggs.[7] Additionally, Tfh cells have been reported to act as precursors of Th2 effector (Th2eff) cells in lung tissue.[9] In contrast to this, multiple studies report no impact on tissue $CD4^+$ Teff cells in the absence of Tfh. It has been shown that IL-21^+ Tfh cells cannot differentiate into IL-4/IL-5/IL-13 producing Th2eff cells, but can mature into IL-21^+ Teff cells.[10] Using a mixed bone marrow chimera model, it has been shown that BCL6 deficient T cells retain the ability to develop into house dust mite (HDM) specific Teff cells in the lung.[11] This is not limited to Th2 cells as Tfh deficient mice showed equivalent frequency and numbers of RSV-specific $CD4^+$ Teff cells in the lung.[12] These studies support the hypothesis that BCL6 dependent Tfh cells do not give rise to Teff cells in the tissue. The view that Tfh and Th2 follow different developmental pathways is supported by the observation that Tfh IL-4 production is regulated by the c-MAF/NFAT pathway, independently of GATA3,[13] explaining why IL-4 expression in Tfh is not perturbed by the

absence of IL-4 signaling.[14] In summary, the differentiation potential of Tfh cells following allergen sensitization and their relative contribution to the pool of tissue Th2eff cells after Type 2 sensitization remains unclear and worthy of further investigation.

The *Il4/Il13* reporter mouse strain (4C13R)[15] was bred to mice which either retained or had deleted the Tfh subset through $CD4^{cre}$-cre/flox specific targeting of BCL6. Local immunization of this novel $BCL6^{fl/fl}$.4C13R.$CD4^{cre}$ strain allowed the number of allergen-induced Th2eff cells that accumulated in tissues to be compared in both the presence and absence of the BCL6-mediated Tfh developmental pathway and to identify what contribution Tfh make to Th2eff responses in the skin and lung.[16]

RESULTS

Tfh development is specifically ablated in $BCL6^{fl/fl}$.$CD4^{cre+/-}$ mice

To investigate the role of Tfh cells in type 2 tissue immune responses, we used an established model of skin Type 2 immunity involving intradermal (i.d.) injection of house dust mite (HDM) allergens into the ear pinna of mice.[16] In this model a significant CD4 T cell response occurs after 7 days in the ear draining auricular lymph node (aLN) and is accompanied by a striking Th2 mediated inflammatory response in the ear tissue.[16] The Tfh cells were identified in the aLN as $CD4^+CD44^{hi}CXCR5^{hi}PD\text{-}1^+$ T cells and non-Tfh were identified as $CD4^+CD44^{hi}CXCR5^-$ T cells (Supplementary figure 1a). Compared with control PBS injected mice, HDM sensitization of the ear pinna triggered a robust proliferation and expansion in the numbers of non-Tfh and Tfh cells in the draining aLN of BCL6 sufficient, $BCL6^{fl/fl}$.$CD4^{cre-/-}$ ($BCL6^{fl/fl}$) mice. By contrast, HDM-sensitized BCL6 deficient, $BCL6^{fl/fl}$.$CD4^{cre+/-}$ ($BCL6^{cKO}$) mice failed to develop any Tfh cells in the draining aLN, while the expansion of the non-Tfh cells was unaffected in these BCL6 deficient mice (Figure 1a, b). Tfh cells are essential for providing "help" to B cells *via* CD40:CD40L signaling to drive B cell activation, maturation and immunoglobulin class switching[3,4] and as expected HDM-sensitized BCL6 sufficient, $BCL6^{fl/fl}$.$CD4^{cre-/-}$ ($BCL6^{fl/fl}$) mice had significantly increased levels of serum IgG1 and IgG2a compared with HDM-sensitized $BCL6^{cKO}$ mice and control PBS injected mice (Figure 1c). These data demonstrate that $CD4^{cre}$-mediated deletion of BCL6 abrogates the development of Tfh cells in the aLN after HDM sensitization in the ear pinna and confirms the essential role of BCL6 in Tfh development in this Th2 model.

Non-Tfh cells show reduced expression of IL-4 in $BCL6^{cKO}$.4C13R mice

To investigate the impact of BCL6 deficiency on the activation of non-Tfh cells in the aLN, we crossed the $BCL6^{fl/fl}$.$CD4^{cre+/-}$ strain onto the 4C13R reporter mouse strain to generate $BCL6^{cKO}$.4C13R mice that lack Tfh cells and report the expression of IL-4 and IL-13 by Th2 cells *via* AmCyan (IL4-AC) and DsRed (IL13-DR), respectively. BCL6 sufficient, $BCL6^{fl/fl}$.4C13R littermates were used as controls. HDM-sensitized BCL6 sufficient mice significantly increased the frequency and total numbers of non-Tfh cells expressing $IL4\text{-}AC^+$ in the draining aLN. However, no $IL13\text{-}DR^+$-expressing non-Tfh cells could be detected in the in the aLN. Interestingly in HDM-immunized BCL6 deficient mice, both the frequency and total count of $IL4\text{-}AC^+$ non-Tfh Th2 cells in the aLN were reduced back to non-sensitized levels (Figure 2a, b). Of note, we failed to detect expression of IL13-DR in Tfh cells in our model, in contrast to previous reports of an $IL\text{-}13^+$ high affinity IgE-promoting Tfh cell.[17,18] We hypothesize this is due to the single-prime sensitization model we employ and suggest that the induction of rare $IL\text{-}13^+$ Tfh cells only occurs in chronic/anaphylactic models of type 2 immunity. When enumerated, these data reveal that non-Tfh and Tfh cell compartments evenly contribute to the $IL\text{-}4^+$ CD4 T cell pool and that this pool is dramatically reduced in $BCL6^{cKO}$ mice after HDM sensitization (Figure 2d).

Taken together our experiments indicate that a clearly defined population of $IL\text{-}4^+$ non-Tfh Th2 cells appears in the aLN after HDM sensitization, which is in contrast to other studies which observe that 100% of $IL\text{-}4^+$ cells in the dLN are Tfh cells.[9] We also show that BCL6 deficiency in CD4 T cells reduces the number of HDM inducible non-Tfh cells that express IL-4.

Skin Th2 effector CD4 cells develop in $CD4^{cre+/-}$.$BCL6^{cKO}$.4C13R mice

To assess the impact of Tfh depletion on Th2 cells in tissues, we looked at the effect of BCL6 deletion on CD4 T cell accumulation in the ear pinnae of HDM-sensitized mice. The CD4 T cells in the ear tissue following allergen sensitization were gated as live, $CD45^+$\$CD64^-Ly6G^-SiglecF^-CD11b^-Ly6C^-TCR\gamma\delta^-CD3^+CD4^+$ cells (Supplementary figure 1b). HDM sensitization triggered a robust CD4 T cell response in the skin tissue of $BCL6^{fl/fl}$ and $BCL6^{cKO}$ mice, compared with control PBS injected mice. Interestingly, the total number of CD4 T cells trended to being increased compared with $BCL6^{fl/fl}$ controls (Figure 3a). We next used the $BCL6^{cKO}$.4C13R mouse strain to investigate the effect of BCL6 deletion on the

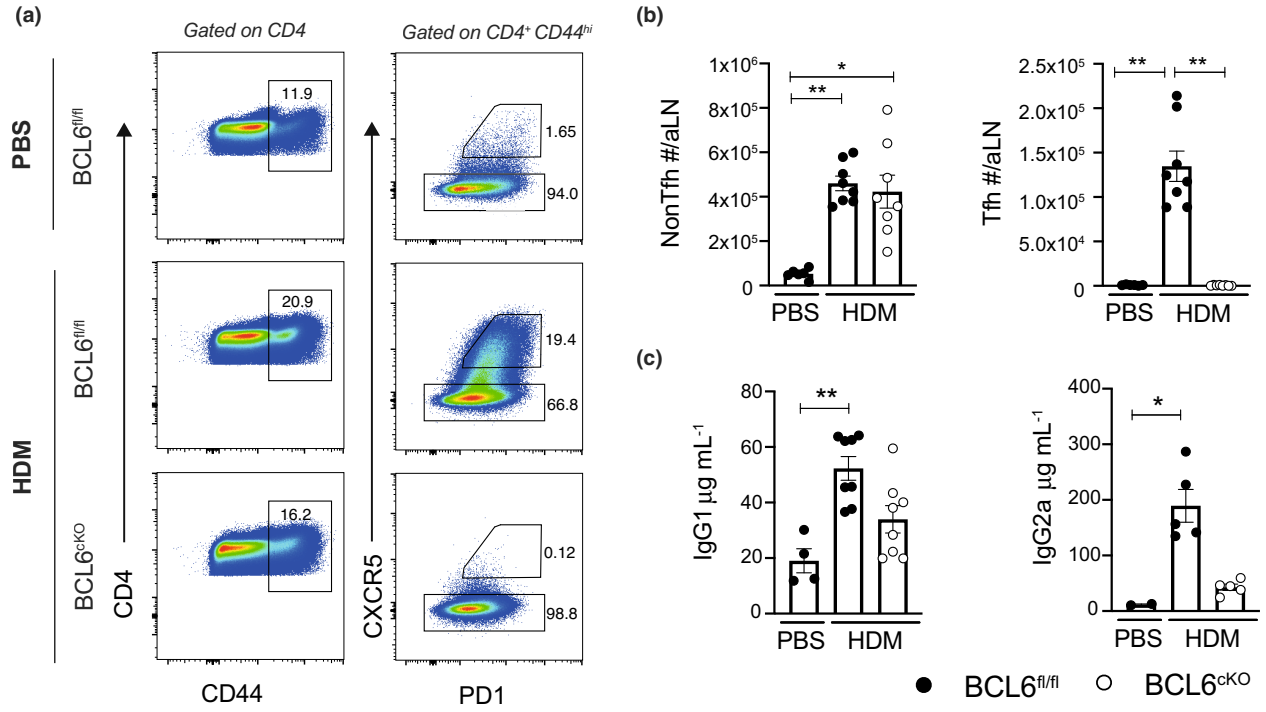

Figure 1. BCL6^{cKO} mice lack Tfh cells, impeding the IgG response. BCL6$^{fl/fl}$ and BCL6^{cKO} mice were sensitized with 200 µg HDM or 30 µL PBS i.d. in the ear pinna. **(a)** Flow cytometry depicting CD44^{hi} CD4 T cells and Tfh/non-Tfh cells by CXCR5 and PD-1 expression day 7 post HDM. **(b)** Total number of CD4^{+}CD44^{hi} non-Tfh (CXCR5^{-}) cells and Tfh cells (CXCR5^{hi}PD1^{+}) in aLN day 7 post HDM. **(c)** IgG1 and IgG2a concentration in serum day 14 post HDM sensitization. Black circles represent BCL6$^{fl/fl}$, white circles represent BCL6^{cKO} samples. Data are shown as mean ± s.e.m. for six ears per group from one of five repeats that gave similar results except for ELISA data which shows five mice per group from one of two repeats. *$P < 0.05$, **$P < 0.01$, not significant is not shown. *P*-values were determined using a Kruskal-Wallis test applying Dunn's multiple comparison post-test.

development of Th2eff subsets expressing IL4-AC^{+} and IL13-DR.[14] The Th2eff subsets that can be detected in the skin of these immunized mice include IL4-AC^{+} single-positive (IL4-AC SP), IL4-AC^{+}IL13-DR^{+} double-positive (IL4-AC.IL13-DR DP), and IL13-DR^{+} single positive (IL13-DR SP) CD4 T cells. The frequency of each of the Th2eff subsets recruited to the ear pinna of HDM-sensitized mice was unaffected in BCL6^{cKO}.4C13R mice compared with BCL6$^{fl/fl}$.4C13R (Figure 3b, c). However, the total count of all three Th2eff subsets were significantly increased due to the modest increase in total CD4 T cell accumulation (Figure 3d). This shows that the lack of Tfh cells in BCL6^{cKO} mice does not impede the development of skin Th2eff cell subsets, suggesting that Tfh cells do not contribute to the Th2eff cell pool in the skin in response to HDM sensitization.

To verify that the CD4 T cells accumulating in the skin of HDM allergen-sensitized mice were derived from the dLN, the egress of lymphocytes was blocked using the sphingosine-1-phosphate (S1P) agonist, FTY720. The recruitment of CD4 T cells to the skin tissue was significantly impaired when mice were treated with FTY720 compared with PBS-treated controls (Figure 3e), indicating that skin CD4 T cells are derived from the aLN.

Taken together, these data show that skin Th2eff cells are primed in the LN, egress and migrate to the skin tissue and that this process is not dependent on a BCL6 mediated step. This suggests that skin Th2eff cells are derived from a non-Tfh precursor that was primed in the draining aLN.

BCL6 deficiency leads to minimal transcriptional changes in skin Th2eff cells

To ensure that the CD4 Th2eff cells appearing in the skin of HDM-immunized BCL6^{cKO}.4C13R mice were unaffected by the BCL6 deficiency, we compared the transcriptional profile of each of the defined Th2eff subsets. Ultra-Low-Input-RNA-seq (ULI-RNA-seq) was performed on purified IL4-AC SP; IL4-AC.IL13-DR DP and IL13-DR SP Th2eff subsets from HDM-sensitized BCL6^{cKO}.4C13R and BCL6$^{fl/fl}$.4C13R control mice and gene expression patterns were compared. Ear tissue was

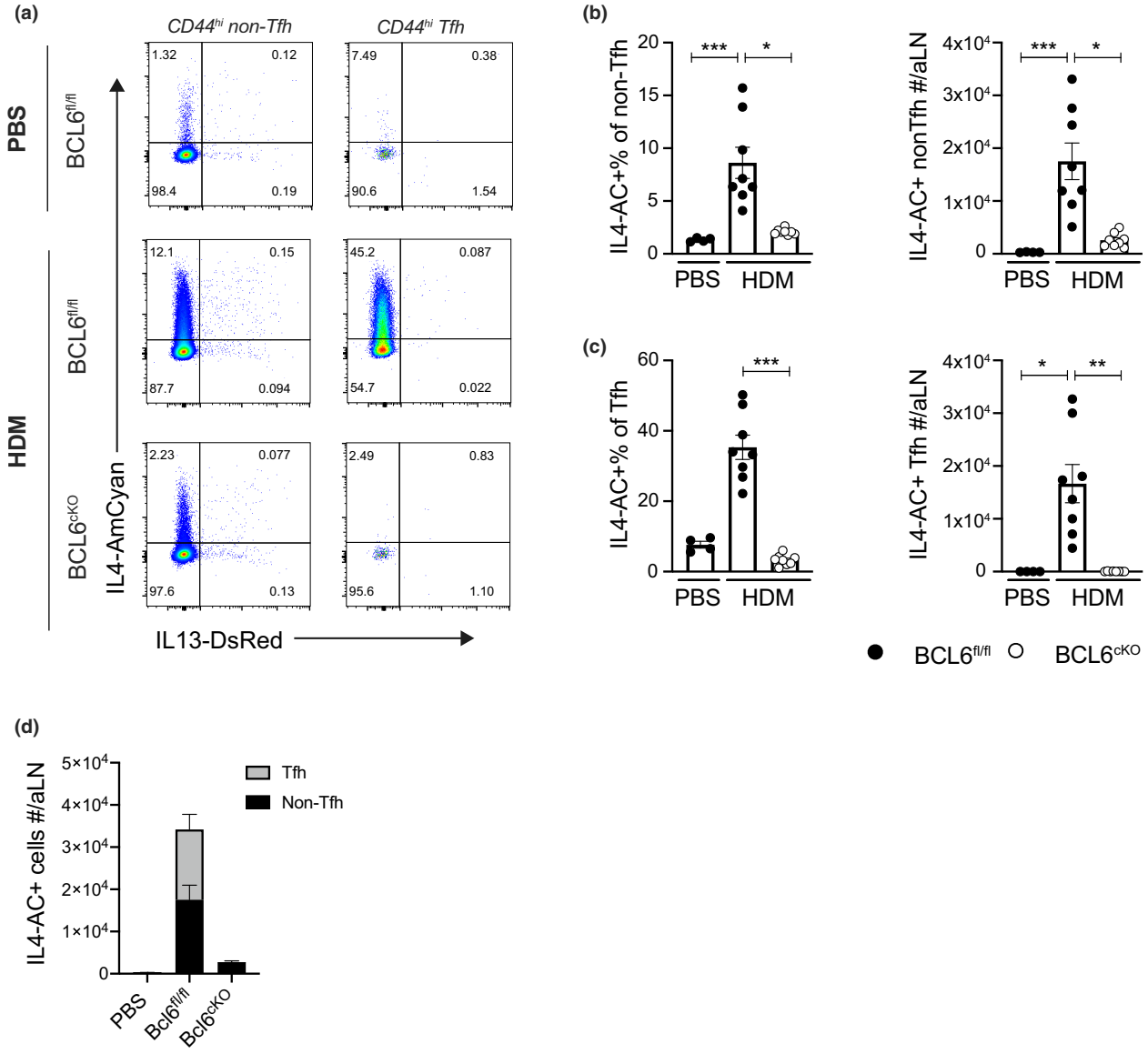

Figure 2. Non-Tfh cells express reduced levels of IL4-AC in BCL6^{cKO}.4C13R mice. BCL6$^{fl/fl}$.4C13R and BCL6^{cKO}.4C13R mice were injected in the ear pinna with 200 μg HDM in 30 μL PBS or PBS alone and cells from the draining aLNs were harvested for analysis on day 7. **(a)** Flow cytometry plots depicting the expression of IL4-AC and IL13-DR in non-Tfh and Tfh cells. **(b, c)** Frequency and total number of IL4-AC^{+} non-Tfh **(b)** and IL4-AC^{+} Tfh cells **(c)**. **(d)** Total number of IL4-AC^{+} non-Tfh and Tfh cells. Black circles represent BCL6$^{fl/fl}$, white circles represent BCL6^{cKO} samples. Data are shown as mean ± s.e.m. for six aLN per group from one of five repeats that gave similar results. *P < 0.05, **P < 0.01, ***P < 0.001, not significant is not shown. P-values were determined using a Kruskal-Wallis test applying Dunn's multiple comparison post-test.

harvested and 1000 cells of each skin Th2eff subset were sorted in triplicate for ULI-RNA-seq transcriptome analysis.[19,20] As CD4 T cells in the ear tissue of naïve mice are rare, naïve CD4 T cells from aLN were sorted and used as a control.

Principal component analysis (PCA) of BCL6^{cKO}.4C13R and BCL6$^{fl/fl}$.4C13R Th2eff subsets revealed that the PC1 axis accounted for 32.1% of the variance primarily based on the distinct Th2eff subsets. IL4-AC SP cells clustered on the left of the PCA plot, whilst IL4-AC.IL13-DR DP and IL13-DR SP subsets fell on the right, suggesting that IL4-AC SP cells are transcriptionally distinct from IL13-DR^{+} cells. The PC2 axis accounted for 15.4% of the variance; however, no meaningful separation was noted *via* PC2. BCL6 sufficiency/deficiency did not influence PCA clustering on the PC1 or PC2 axis; however, samples did segregate based on BCL6 genotype on the PC3 axis that accounted

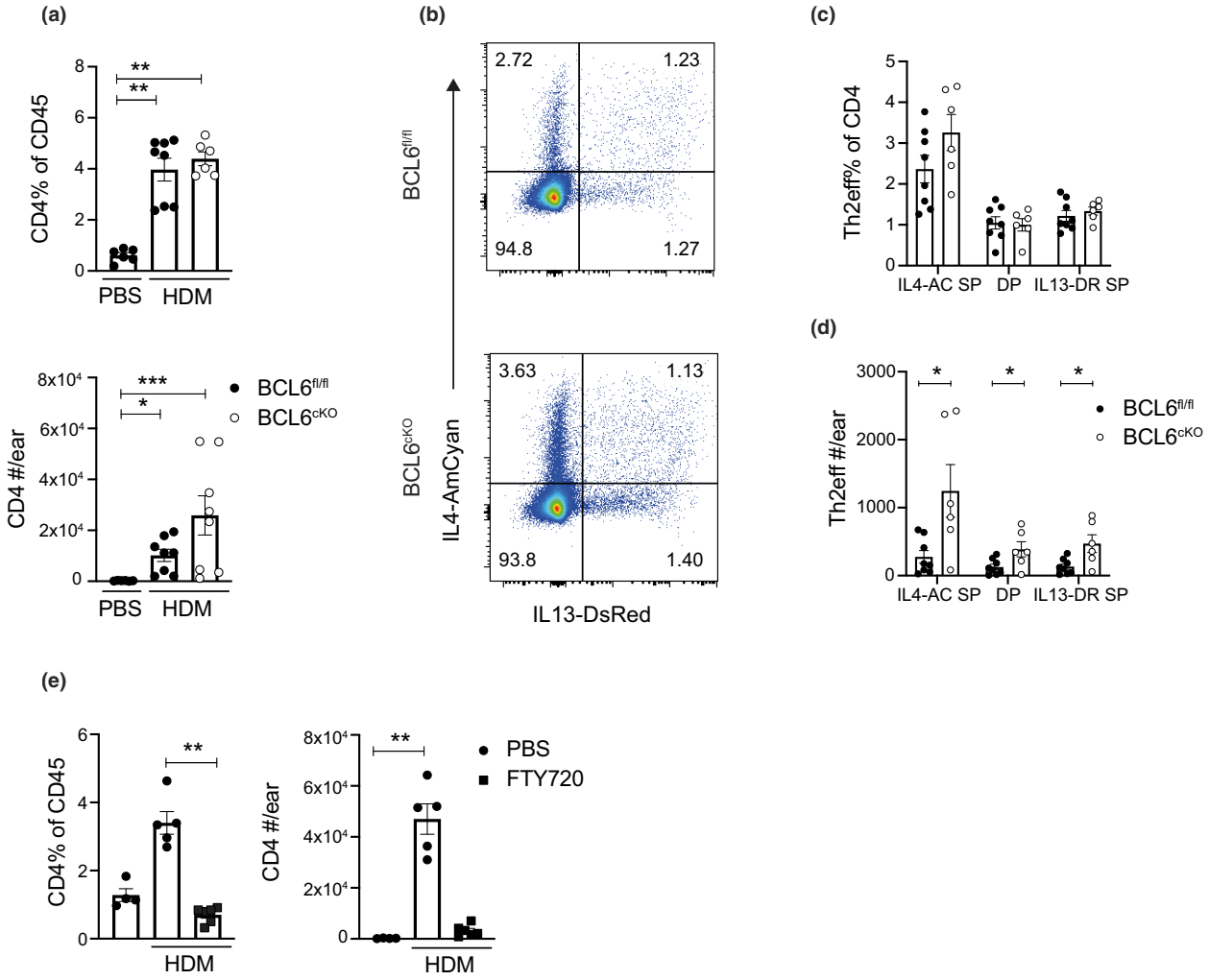

Figure 3. Skin Th2eff develop independently of Tfh cells. Mice were sensitized with injected in the ear pinna with 200 μg HDM in 30 μL PBS or PBS alone. Ear skin tissue was collected for analysis on day 7. **(a)** Frequency and total number of CD4 T cells in ear tissue from BCL6$^{fl/fl}$.4C13R and BCL6^{cKO}.4C13R mice. **(b)** Flow cytometry plots depicting the expression of IL4-AC and IL13-DR in CD4 T cells from BCL6$^{fl/fl}$.4C13R and BCL6^{cKO}.4C13R mice. **(c)** Enumerated frequencies and **(d)** total number of Th2eff cell subsets from BCL6$^{fl/fl}$.4C13R and BCL6^{cKO}.4C13R mice. **(e)** Frequency and total number of CD4 T cells from C57Bl/6J naïve control mice and mice that were injected with 25 μg FTY720 in PBS or PBS alone on days 2 and 4 post HDM sensitization. Black circles represent BCL6$^{fl/fl}$, white circles represent BCL6^{cKO} samples. Data are shown as mean ± s.e.m. for six ears per group from one of five repeats that gave similar results. *$P < 0.05$, **$P < 0.01$, ***$P < 0.001$. *P*-values for **a** and **e** were determined using a Kruskal-Wallis test applying Dunn's multiple comparison post-test. *P*-values for **c** and **d** were determined using a Mann–Whitney *U*-test, independently for each Th2eff subset.

for 9.8% of the variation between samples. BCL6$^{fl/fl}$ samples clustered at the top of the PC3 axis BCL6^{cKO} samples that clustered at the bottom (Figure 4a). This analysis reveals that the primary influence on the transcriptional profile of Th2eff cell subsets was the expression of IL13-DR, followed by the absence/presence of BCL6.

To assess the specific transcriptional regulation of BCL6 in each Th2eff cell subset, the expression of core genes associated with a Th2 phenotype were compared between BCL6^{cKO}.4C13R and BCL6$^{fl/fl}$.4C13R littermate controls (Figure 4b). Expression values were normalized against gene length and represented as "variance stabilized transcripts per kilobase" (VSTpk). Naïve CD4 T cells isolated from aLN were used as controls. All skin Th2eff cells showed increased expression of key Th2 genes compared with naïve aLN control CD4 T cells. Importantly, *Gata3* expression was increased in all Th2eff subsets compared with naïve LN CD4 T cells, indicating that skin Th2eff cells represent the conventional Th2eff subset. Despite the critical role of STAT6 in Th2 cell development, *Stat6* was similarly expressed in naïve and

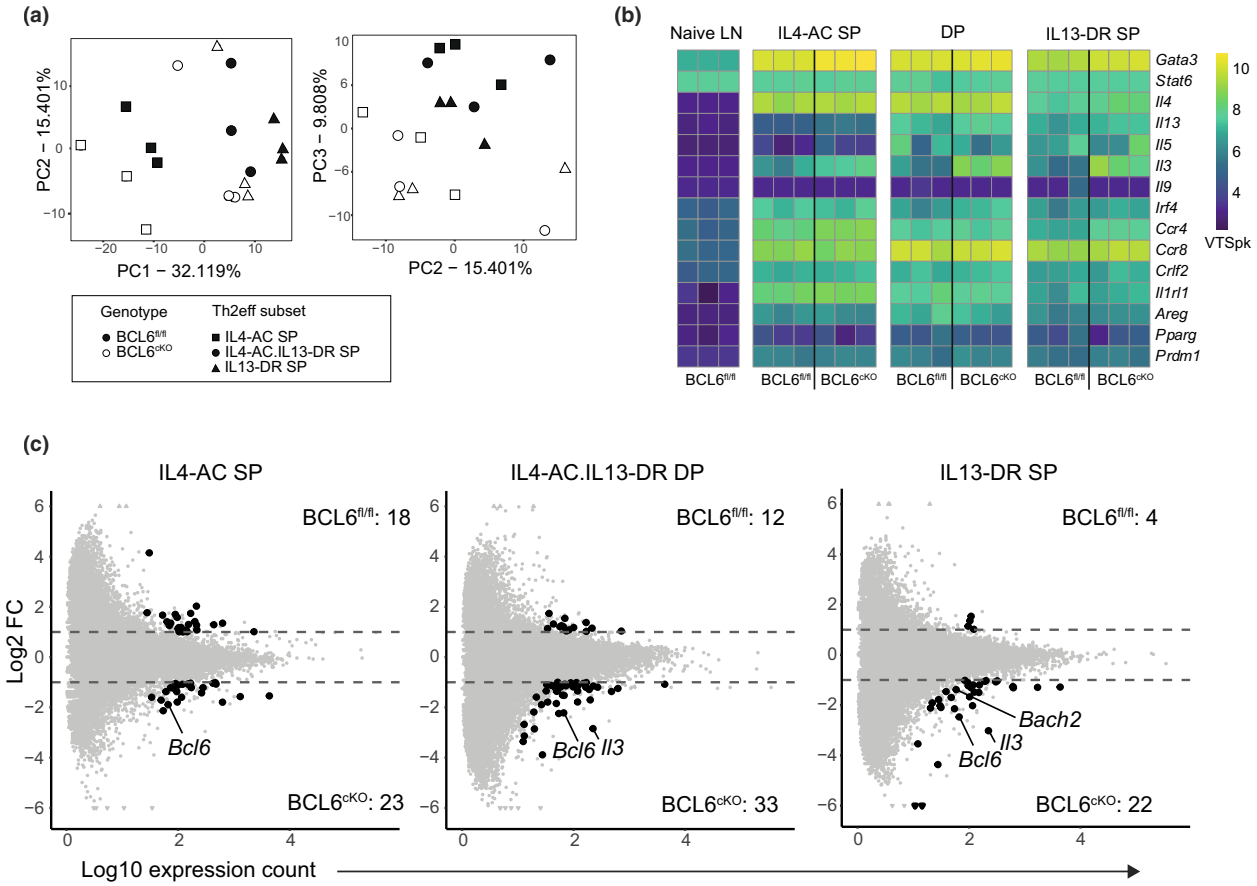

Figure 4. BCL6 deficiency causes minimal transcriptional changes in skin Th2eff cells. Skin Th2eff subsets from BCL6$^{fl/fl}$.4C13R and BCL6^{cKO}.4C13R mice were harvested from draining aLN and sorted 7 days after HDM sensitization and ULI-RNAseq was performed. **(a)** PCA of skin Th2eff subsets, performed on top 1000 highest variance genes for PC1/PC2 and PC2/PC3 axis. BCL6$^{fl/fl}$ samples = black; BCL6^{cKO} samples = white; IL4-AC SP = square; IL4-AC.IL13-DR DP = circle; IL13-DR SP = triangle. **(b)** Heatmap showing VSTpk values of canonical Th2 genes in skin Th2eff subsets and naïve LN CD4 T cells. **(c)** MA plots of skin Th2 subsets comparing BCL6$^{fl/fl}$.4C13R and BCL6^{cKO}.4C13R samples. Black dots represent DEGs with a $\log_2$ FC > 1 or > −1; *P*-value < 0.05; and minimum mean read count > 30. Gray dots do not meet differential expression statistical thresholds.

Th2eff cells. This is not of concern given that *Stat6* mRNA expression does not represent active phosphorylated STAT6. *Il4* was expressed highly in both IL4-AC SP and IL4-AC.IL13-DR DP subsets and was expressed at relatively low levels in the IL13-DR SP subsets and not expressed at all in naïve LN cells. *Il13* was expressed highly in IL13-DR SP and IL4-AC.IL13-DR DP subsets and expressed at low to undetectable levels in IL4-AC SP cells and naïve LN CD4 T cells respectively. Other core Th2 genes including *Il5, Il3, Irf4, Ccr4, Ccr8, Crlf2, Il1rl1, Areg, Pparg* and *Prdm1* were upregulated in all some, if not all, skin Th2eff cell subsets compared with naïve LN controls. Interestingly, *Il9* was not detected in any sample, indicating that IL-9 is not associated with Th2eff cells in our models. Of note, *Il5* expression was increased in IL13-DR^{+} Th2eff subsets, compared with IL4-AC SP cells, indicating the linked association between the expression of *Il13* and *Il5* in skin Th2eff cells.[21–23] These results indicate that IL4-AC and IL13-DR reporter expression in 4C13R mice accurately reflects the endogenous *Il4* and *Il13* gene expression and that all cell subsets sequenced represent bonafide Th2eff cells.

To investigate the impact of BCL6 deficiency on skin Th2eff cells in more depth, differential gene expression analysis was performed on the RNA-seq data comparing BCL6$^{fl/fl}$ and BCL6^{cKO} samples for each Th2eff subset. Differentially expressed genes (DEGs) were defined as having a $\log_2$-fold change (FC) > 1 or < −1, a *P*-value < 0.05 and a minimum mean count > 30. This analysis resulted in less than 50 DEGs between BCL6$^{fl/fl}$ and BCL6^{cKO} samples for each Th2eff subset comparison (Figure 4c, Supplementary tables 1–3), indicating that BCL6 deficiency has a minor effect on the transcriptional profile of Th2eff cells appearing in the skin after HDM

sensitization. BCL6 deficiency triggered the upregulation of more genes in Th2eff subsets than downregulation, supporting the role of BCL6 as a transcriptional repressor in Th2eff cells. The expression of *Bcl6* was significantly upregulated in all Th2eff subsets of BCL6 deficient BCL6^{cKO}.4C13R mice (Figure 4c). Furthermore, intranuclear transcription factor staining shows that BCL6 is also significantly upregulated at the protein level in BCL6^{cKO}.4C13R mice (Supplementary figure 2a, b). The increased level of *Bcl6* reads in BCL6^{cKO} samples has been previously shown to be due to the negative autoregulation of *Bcl6*.[24] Supplementary figure 2c shows that the increased *Bcl6* reads map to exons 1–6 and exon 10, not exons 7–9, which are selectively excised by CD4^{cre} mediated targeting in BCL6^{cKO} mice.[25] This validates the flox/cre system. *Bcl6* exons 7–9 encode several critical zinc finger motifs that mediate DNA binding, therefore the deletion of exons 7–9 results in a dysfunctional BCL6 protein that is reflected by the absence of Tfh cells. Therefore, the loss of functional BCL6 protein promotes enhanced transcription of *Bcl6*, resulting in increased *Bcl6* RNA-seq reads in BCL6^{cKO} samples. *Bach2* and *Il3* were also significantly upregulated in BCL6^{cKO} IL13-DR^{+} Th2eff subsets (Figure 4c), indicating that BCL6 represses the expression of these genes.

Recruitment of type 2 granulocytes is increased in BCL6^{cKO}.4C13R mice

IL-3 is a canonical type 2 cytokine expressed by effector Th2 cells and is crucial for basophil recruitment and eosinophil survival.[26,27] The observation that *Il3* mRNA was increased in Th2eff samples from BCL6^{cKO}.4C13R mice led us to investigate whether there was an associated basophil and eosinophil response in our skin HDM model. Strikingly, both basophils and eosinophils in the ear tissue were significantly enriched in BCL6^{cKO}.4C13R mouse ear tissues after HDM sensitization compared with BCL6$^{fl/fl}$.4C13R counterparts at all time points analyzed (Figure 5a). Furthermore, the MFI of the activation marker CD11b[28,29] was not affected in BCL6^{cKO}.4C13R and BCL6$^{fl/fl}$.4C13R controls (Figure 5b). This demonstrates that allergen activation of BCL6 deficient CD4 T cells triggers an enhanced recruitment of basophils and eosinophils into the skin tissue, but their activation as defined by CD11b upregulation was not affected.

In CD4^{+} Th2 cells, the transcription factor GATA3 has well-defined roles in Th2 differentiation and cytokine expression.[30] However, it has also been shown to play a critical role in promoting the expression of FOXP3 and functional suppressive activity in Treg cells.[31] In this regard the Th2 cytokine-promoting activity of GATA3 must be tightly regulated in Treg cells to prevent the expression of GATA3-dependent Th2 genes. BCL6 has been shown to be a critical regulator of GATA3 function in Tregs where BCL6 deficient Treg cells show increased expression of GATA3 and Th2 cytokines, resulting in enhanced Th2 inflammation.[32,33] This raised the possibility that enhanced eosinophil and basophil infiltration in BCL6^{cKO}.4C13R mice could be due to the indirect effect of BCL6 deficiency on Treg function. To test this, BCL6^{cKO} and BCL6$^{fl/fl}$ mice were sensitized with HDM in the ear pinna and the frequency of Tregs compared in each mouse strain using intranuclear FOXP3 staining and flow cytometry. The frequency of Treg cells in the ear tissue was significantly decreased in BCL6^{cKO} mice compared with BCL6$^{fl/fl}$ littermate controls; however, due to the increased number of CD4 T cells the total number of Treg cells appearing in the ears of BCL6^{cKO} mice was not significantly perturbed (Figure 5c). The MFI of GATA3 was slightly increased in BCL6^{cKO}-Treg cells, compared with BCL6$^{fl/fl}$ controls (Figure 5d). These data support the finding that BCL6 normally suppresses GATA3 in Treg cells to limit the expression of Th2 genes. In addition to the increased Th2eff cell numbers in the skin of BCL6^{cKO} mice, the Th2-skewing of Treg cells provides another factor that may contribute to the enhanced recruitment of eosinophils and basophils in the skin tissue of BCL6^{cKO} mice.

Lung Th2eff cells are reduced in BCL6^{cKO}.4C13R mice after primary *Nippostrongylus brasiliensis* infection

Given previous findings that IL-4^{+} Tfh cells can give rise to Th2eff cells in the lung,[9] we next employed a lung model of Type 2 immunity and tested the dependency of lung Th2eff cells on Tfh cells. BCL6^{cKO}.4C13R and BCL6$^{fl/fl}$.4C13R littermate controls were infected subcutaneously with 550 live *Nb* L3 larvae or PBS, and the lung draining mediastinal lymph node (medLN) and lung tissue were analyzed to determine the frequency of Th2eff in the lung. Cellular responses were analyzed on day 10 post-*Nb* infection, at the peak of the Th2 CD4 response to this stimulus.[34,35] As seen in the HDM skin sensitization model, the development of Tfh cells in the medLN was completely inhibited in the BCL6^{cKO}.4C13R mice, whilst the number of non-Tfh cells was similar to the BCL6$^{fl/fl}$.4C13R controls (Figure 6a, b). Live *Nb* infection triggered a robust increase in the frequency and total number of IL4-AC^{+} non-Tfh cells compared with the PBS controls and this trended to being decreased in BCL6^{cKO}.4C13R mice (Figure 6c, d). Compared with the PBS controls, Tfh cells in *Nb* infected mice significantly upregulated the expression of IL4-AC and due to the complete ablation of Tfh cells, this population was absent in BCL6^{cKO}.4C13R mice

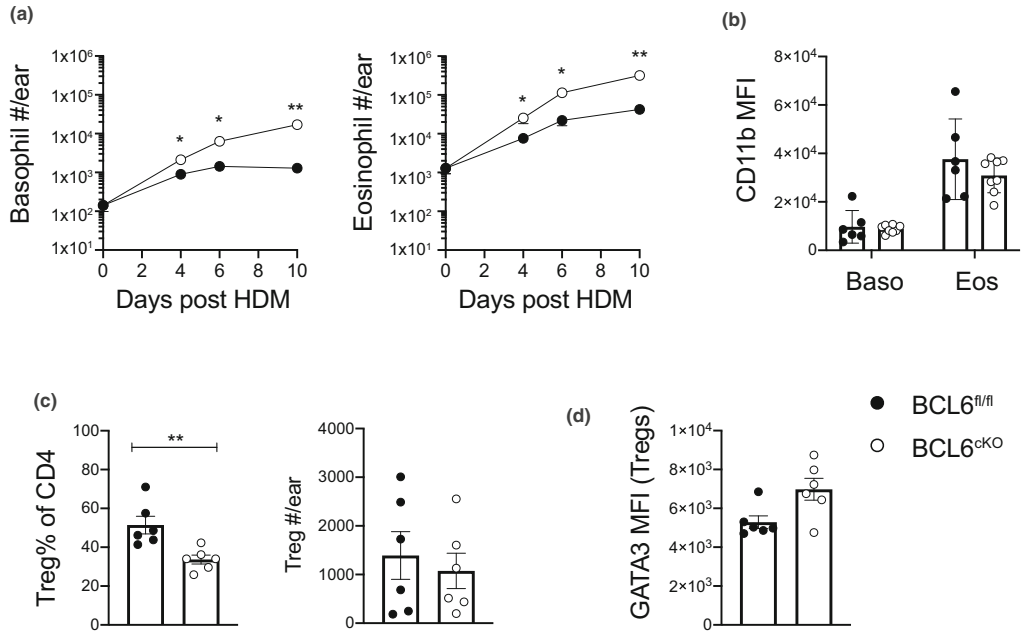

Figure 5. Basophil and eosinophil recruitment to the skin is enhanced in BCL6^{cKO}.4C13R mice and correlates to reduced frequency of Treg cells. BCL6$^{fl/fl}$.4C13R and BCL6^{cKO}.4C13R mice injected in the ear pinna with 200 μg HDM in 30 μL PBS or PBS alone. Ear skin tissue was collected for analysis on day 7 unless indicated. **(a)** Kinetics of total number of basophils and eosinophils detected in ear tissue. **(b)** CD11b MFI in basophils and eosinophils. **(c)** Frequency and total number of FOXP3^{+} Treg cells in ear tissue. **(d)** GATA3 MFI in FOXP3^{+} Treg cells in ear tissue. Black circles represent BCL6$^{fl/fl}$, white circles represent BCL6^{cKO} samples. Data are shown as mean ± s.e.m. for six ears per group from one of five repeats that gave similar results. *P < 0.05, **P < 0.01. P-values were determined using a Mann–Whitney U-test.

(Figure 6c, e). These results indicate that as observed in the skin HDM sensitization model, a significant population of IL-4 producing non-Tfh appears in the medLN following *Nb* infection. Furthermore these data agree with the aLN/skin data that the loss of Tfh cells and/or the loss of intrinsic BCL6 regulation reduces the frequency of IL-4 producing non-Tfh cells.

The frequency of lung infiltrating CD4 T cells was increased approximately 2-fold in *Nb* infected mice compared with PBS controls and this was not affected by BCL6 deficiency in BCL6^{cKO}.4C13R mice compared with BCL6$^{fl/fl}$.4C13R controls (Figure 6f). The frequencies of all three Th2eff subsets were significantly decreased in BCL6^{cKO}.4C13R mice (Figure 6g, h), indicating that BCL6 may have a role in the development of Th2eff in the lung. This contrasts with the HDM skin sensitization data which showed no role for Tfh cells in skin Th2eff development (Figure 3b–d), indicating that tissue-specific regulation may distinguish the role of Tfh cells in skin and lung type 2 effector responses.

DISCUSSION

We describe the use of a conditional CD4, BCL6 deficient *Il4/Il13* reporter mouse strain to examine the contribution that the Tfh subset makes to the development of Th2eff cells in the skin and lung. We report that Tfh cells do not contribute to Th2eff cell development in the skin as comparable numbers of all three *Il4* and *Il13* expressing Th2eff subsets develop in the skin of HDM sensitized BCL6 sufficient and BCL6/Tfh-deficient mice. This conclusion is consistent with Lonnberg *et al.*[36] who showed an early bifurcation of Th1 and Tfh cells from a common precursor in spleen CD4 T cells in malaria-infected mice and reported no evidence of functional plasticity once the commitment to a T helper cell fate had been established.

One potential limitation of the BCL6^{cKO} mice used in our study is the observation that BCL6 could potentially regulate gene expression in non-Tfh CD4 T cell compartments such as Th2 cells and other non-Th2 cells including Tregs. By using RNA-seq we showed that despite its prominent role as a transcriptional repressor, BCL6 does not play a significant role in the intrinsic regulation of allergen-primed skin Th2eff cells. This was evident from differential gene analysis that resulted in less than 50 DEGs between BCL6 sufficient and deficient cells, for each Th2eff cell subset. Of note, *Bach2* was one of the 22 genes upregulated in BCL6^{cKO} IL13-DR SP samples. BACH2 is a transcriptional repressor that has been

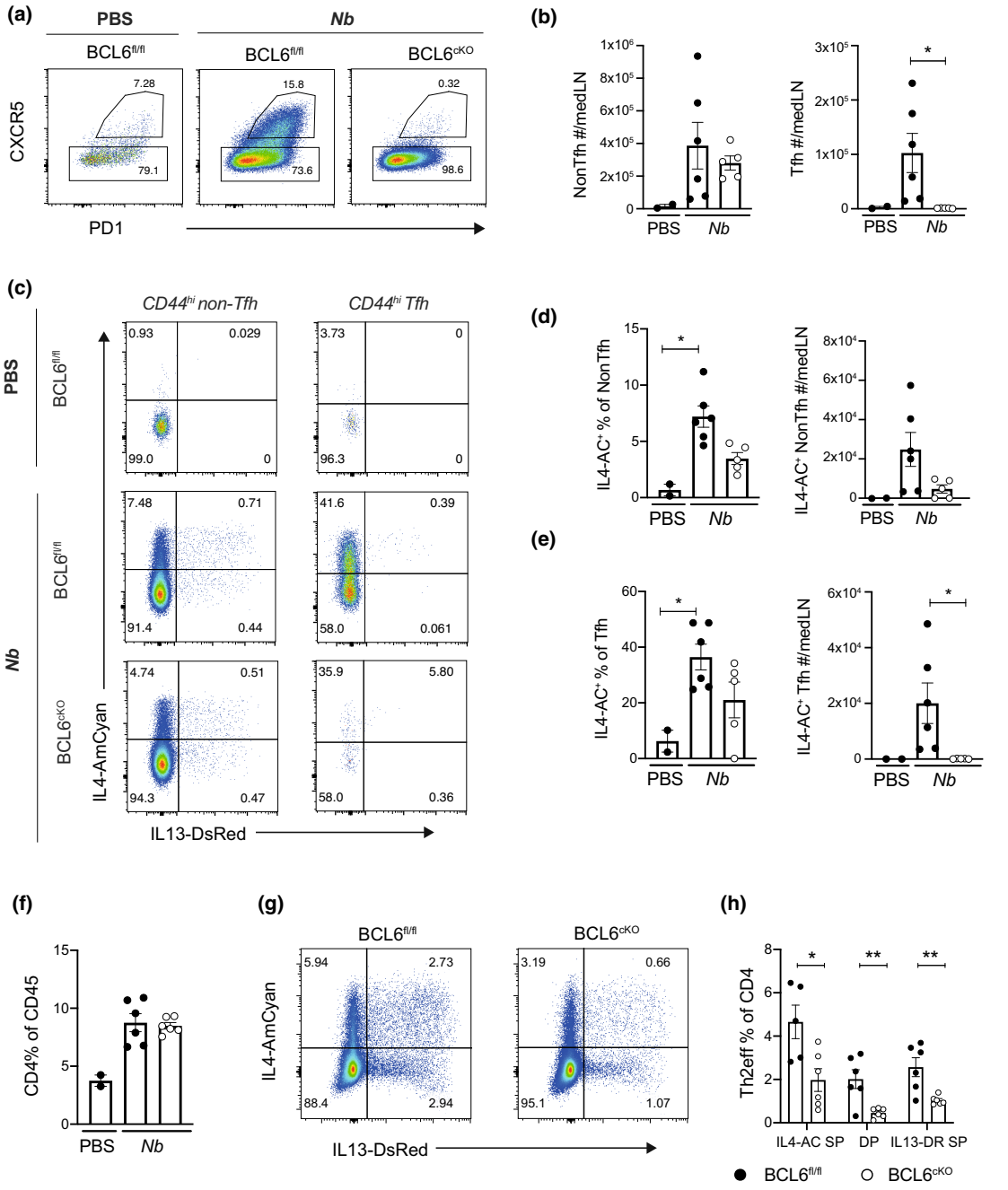

Figure 6. BCL6^{cKO}.4C13R mice show a partial dependence on Tfh cells for Th2eff cell development in the lung. BCL6$^{fl/fl}$.4C13R and BCL6^{cKO}.4C13R mice were infected with 550 live *Nb* L3 subcutaneously in neck scruff. Lung and draining LN tissues were collected and cells harvested for analysis on day 10. **(a)** Flow cytometry plots gated on CD4^{+} CD44^{hi} depicting expression of CXCR5 and PD1 to identify Tfh and non-Tfh cells. **(b)** Total number of non-Tfh and Tfh cells in medLN. **(c)** Flow cytometry plots depicting the expression of IL4-AC and IL13-DR in non-Tfh and Tfh cells in the medLN. **(d, e)** Frequency and total number of IL4-AC^{+} non-Tfh **(d)** and IL4-AC^{+} Tfh cells **(e). (f)** Frequency of CD4 T cells in the lung. **(g)** Flow cytometry plots depicting IL4-AC and IL13-DR expression in lung CD4 T cells. **(h)** Frequencies of Th2eff subsets in the lung tissue. Black circles represent BCL6$^{fl/fl}$, white circles represent BCL6^{cKO} samples. Data are shown as mean ± s.e.m. for 2–6 mice per group from one of two repeats that gave similar results. **P* < 0.05, ***P* < 0.01. *P*-values were determined for **b** an **d**–**f** using a Kruskal-Wallis test applying Dunn's multiple comparison post-test. *P*-values for **h** were determined using a Mann–Whitney *U*-test, independently for each Th2eff subset.

shown to inhibit Th2 differentiation.[37] BACH2 inhibits BLIMP-1,[38] an antagonistic partner of BCL6. Therefore, the upregulation of *Bach2* in BCL6^{cKO} IL13-DR SP cells may represent a feedback loop whereby BACH2 indirectly promotes the expression of BCL6 through repression of BLIMP-1 in BCL6 deficient cells. However, despite altered *Bach2* expression, the limited transcriptional differences suggests the functional expression of BACH2 was not substantially altered in the absence of BCL6. It is possible that the lack of BCL6 transcriptional repression in BCL6^{cKO} Th2eff cells may lead to enhanced IL-4 and IL-13 expression, concealing the loss of Tfh-derived Th2eff cells in our experiments. However, if this were the case, we would expect to see increased expression of *Il4* and *Il13* in BCL6^{cKO} Th2eff cells. RNA-seq analysis did reveal that *Il13* was significantly upregulated in BCL6^{cKO} IL4-AC SP cells; however, given that IL4-AC SP cells do not express IL13-DR, this upregulation of *Il13* was not substantial enough to induce DsRed expression from the 4C13R transgene. Furthermore, the expression of *Il13* in IL4-AC SP BCL6^{cKO} cells remained substantially lower than IL13-DR^{+} counterparts. In summary, the overall lack of intrinsic BCL6 regulation in skin Th2eff cells negates the possibility that Th2 deficiency in the skin is masked. Instead these results give confidence to our conclusion that Th2eff cells are derived from non-Tfh cells in the aLN and not Tfh cells.

Interestingly, we did observe that BCL6 regulation could occur in the Treg compartment as seen by a reduction in the frequency of Treg cells in the skin accompanied by increased expression of GATA3 in Treg cells from BCL6^{cKO} mice. We hypothesize this contributes to the enhanced infiltration of eosinophils and basophils observed in the skin tissue. Increased eosinophil and basophil recruitment has been reported in germline BCL6 KO mice, although it was attributed to BCL6-dependent suppression of chemokine expression in macrophages.[39,40] Here, we provide evidence that BCL6 acts to suppress the GATA3-dependent Th2 program in Treg cells, which we postulate aids the regulatory function of Treg cells and limits the recruitment of eosinophils and basophils to the skin tissue. In addition to Tregs, BCL6 deficient IL4-AC.IL13-DR DP and IL13-DR SP Th2eff cells upregulated *Il3* compared with BCL6 sufficient counterparts. This enhanced *Il3* expression, along with the general increase in total numbers of Th2eff cell subsets, due to increased CD4 T cell counts, may also contribute to the increased recruitment of eosinophils and basophils to the tissue.

In the two models of type 2 immunity employed in this study, we report that approximately half of IL-4^{+} CD4 T cells in the aLN are of the Tfh lineage and that the frequency of IL-4^{+} non-Tfh cells is reduced in BCL6^{cKO} mice. Therefore, the loss of Tfh cells results in a substantial decrease of IL-4 availability in the aLN, which may explain the reduced frequency of IL-4^{+} non-Tfh "classical" Th2 cells, given the critical role of IL-4 in Th2 differentiation. T helper cell differentiation is thought to take place in the draining lymph node, alongside MHC-II/TCR mediated activation of naïve CD4 T cells by dendritic cells, and is dependent on the cytokines present in the environmental milieu of the lymph node at the time of activation.[41] The allergen induced Th2eff cells appearing in the tissues are thought to be derived from IL-4^{+} non-Tfh Th2 cells in the aLN. However, our analysis of skin Th2eff cells indicates that the reduction of Th2 cells in aLN of BCL6^{cKO} mice does not result in reduced numbers of skin Th2eff cells. This is most probably related to LN output of Th2 cells capable of migrating to tissues and becoming Th2eff, which is more than able to fill the available inflammatory niches at the sensitized skin site in the ear pinna.

The observation that Th2eff cells were reduced in the lungs of Tfh-deficient BCL6^{cKO}.4C13R mice by approximately 2-fold in response to a live *Nb* infection leaves open the possibility that Th2eff cells in the lung may be partially derived from Tfh cells in the medLN. This supports a previous finding by Ballesteros *et al.*[9] who reported that 100% of IL-4^{+} cells in the medLN were Tfh cells and that inhibition of Tfh cells using a BCL6 inhibitor reduced the development of both IL-4^{+} and IL-13^{+} Th2eff cells in the lung tissue by approximately 3-fold. Alternatively, the lung may not hold a maximum niche for Th2eff cells like the skin, and thus if medLN non-Tfh Th2 cells are the precursors to Th2eff cells in the lung, the reduction of IL-4^{+} non-Tfh Th2 cells would directly translate to the reduced Th2eff cells observed in the lung. Given that Ballesteros *et al.* did not detect IL-4^{+} non-Tfh cells in the medLN, this alternate hypothesis of non-Tfh derived Th2eff cells in the lung does not apply to their chronic, recall challenge model of HDM-induced lung inflammation. Given the complex nature of the lung microenvironment, the difficulty of accurately enumerating cell numbers, and model specific differences, further studies will be required to determine whether Tfh cells play a role in lung Th2eff cell development.

In summary, our data show that Tfh are not necessary for the differentiation of Th2eff cells in a primary HDM sensitization model in the skin; however, in a chronic lung type 2 model a partial Tfh-dependent Th2eff response may occur, but not as significantly as reported elsewhere. This work supports the hypothesis that allergen activated Tfh cells diverge early in the CD4 T cell differentiation pathway and represent a distinct subset of CD4 T cells in the aLN that do not contribute to the pool of Th2eff cells that are activated and migrate to the

skin. Additionally, we report that BCL6 normally acts to suppress CD4 T cell mediated type 2 inflammatory response in the skin, with increased eosinophil and basophil infiltration in BCL6^{cKO} mice. We suggest that this is due to a number of contributing factors, including the regulatory role of BCL6 in maintaining Treg function through inhibition of the GATA3 induced Th2 genes. We support the notion that BCL6 does not influence Th2eff cell differentiation despite its obligatory role in Tfh development, and indicate that primary skin Th2eff cells are derived from a non-Tfh precursor in the lymph node.

METHODS

Mice

All mice were bred and maintained on a C57BL/6 background in a specific pathogen-free barrier conditions in the Malaghan Institute of Medical Research Biomedical Research Unit. The 4C13R[15] reporter mice bacterial artificial chromosome does not interfere with normal immune function with similar levels of T cells, B cells, immunoglobulin and inflammatory cells being induced by immunization compared with wild type C57BL/6 mice. Bcl6$^{fl/fl}$ and CD4^{cre} strains were imported from the John Curtin School of Medical Research, ANU, Canberra. All animal procedures were approved by the Victoria University of Wellington Animal Ethics committee and performed in accordance with institutional guidelines.

Immunizations and treatments

Mice were anesthetized using xylazine and ketamine (Phoenix, Auckland, New Zealand). 30 μL of a solution containing 200 μg HDM (Greer Laboratories, Lenoir, NC, USA) was injected intradermally into the ear pinna and mice were killed 7 days later. For live *Nippostrongylus brasiliensis* infections, the mice were injected with 550 L3 larvae subcutaneously in the scruff of the neck and killed 10 days later. To block egress of cells from lymph nodes the mice were treated with 25 μg FTY720 in PBS intra-peritoneally at day 2 and again on day 4 after HDM immunization.

Cell isolation and flow cytometry

Draining lymph nodes were pressed through a 70-μm cell strainer into complete media [IMDM (Gibco, ThermoFisher Scientific, MA, USA) supplemented with 5% FBS (Sigma-Aldrich, MO, USA), 100 U mL^{-1} penicillin per 100 μg mL^{-1} streptomycin (Invitrogen™, ThermoFisher Scientific, Waltham, MA, USA) and 55 μM β-mercaptoethanol (Invitrogen, Waltham, MA, USA) to make a single cell suspension. Dorsal and ventral ear sheets were separated and minced into very fine pieces using scissors. Each ear was digested in 3 mL digestion media [IMDM (Gibco), containing 1.2 mg collagenase IV (Sigma) and 120 μg mL^{-1} DNAse I (Roche, Basel, Switzerland)] and incubated in a 37°C shaking incubator at 200 rpm for 30 min. Ear wash buffer [PBS containing 1% BSA (Sigma, St Louis, MO, USA) and 5 mM EDTA (Invitrogen)] was added immediately to stop the digestion. The solution was pipetted up and down to further dissociate tissue and passed through a 70-μm cell strainer. The ears were washed once more in ear wash buffer then red blood cells were lysed using ammonium-chloride-potassium buffer [1 mM EDTA (Invitrogen), 150 mM NH_4Cl (Sigma), 10 mM $NaHCO_3$ (Sigma) in ddH_2O] before being resuspended in complete media. Half the lung was taken and used for digestion. Briefly, the lungs were finely minced and digested in 2 mL digestion media [DMEM (Gibco), containing 2.4 mg mL^{-1} Collagenase I (Sigma) and 120 μg mL^{-1} DNAse I (Roche)] for 1 h in a 37°C shaking incubator at 200 rpm. The solution was pipetted up and down to further dissociate tissue and passed through a 70-μm cell strainer. Lungs were washed in complete media before being counted and stained for flow cytometry. Live cell counts were performed using a hemocytometer and trypan blue (Invitrogen) exclusion. For FACS analysis, the cells were resuspended in FACS buffer [2% FBS (Sigma), 1 mM EDTA (Invitrogen), 0.01% sodium azide (Sigma) in PBS] and 2×10^6 cells were plated for staining. The cells were first incubated with anti-CD16/32 antibody (clone 2.4G2) before staining with fluorophore-conjugated antibodies. Lymph node samples were stained for CXCR5 (2G8, Biotin) at 37°C for 30 min separately from full antibody cocktail mix. Cell surface antibody cocktails were made up using combinations of: SiglecF-BV421, CD11b-BV570, CD90.2-BV605, CD90.2-PECy7, NK1.1-BV650, Ly6G-BV711, CD3-PECy5, CD3-BV786, CD8-BV786, CD8-PECy7, CD8-AF700, CD8a-FITC, CD4-PerCPCy5.5, CD4-APCH7, CD4-BV605, CD4-APCCy7, cKit-BB700, CD64-PE dazzle-594, CD49b-PECy7, CD49b-FITC, CD200R3-APC, CD45-APCCy5.5, Ly6C-AF700, PD1-PerCPef710, CD44-AF700, CD44-PECy5, TCRgd-PECy7, CD19-APCH7 and Streptavidin-BV605 (BioLegend, San Diego, CA, USA). The cells were either stained for viability with Zombie-NIR fixable dye prior to 24G2 blocking in PBS, or after cell surface staining with DAPI. Data were acquired on a Cytek Aurora Spectral flow cytometer (Cytek Biosciences, Fremont, CA, USA). Flow data were analyzed using FlowJo software (Treestar).

ELISA and Legendplex

IgG1 and IgG2 serum ELISAs were performed using Invitrogen kits Cat # 88–50 410 and 88–50 420 respectively.

RNA sequencing

Wild type 4C13R or BCL6^{cKO}.4C13R reporter mice were immunized with HDM as above, killed on day 7 and the Th2 effector subsets isolated from ear tissue were sorted for using a BD Influx cell sorter. Th2eff cell subsets were gated as CD45$^+$, CD3^{int,} TCRγd$^-$, CD4$^+$, CD8$^-$ and subsequently either IL4-AC SP, IL4-AC.IL13-DR DP or IL13-DR SP. CD4$^+$ cells from naïve aLN were also sequenced as a control. 1000 cells were sorted directly into 5 μL lysis buffer [TCL Buffer (Qiagen, Hilden, Germany)] with 1% 2-mercaptoethanol), Smart-seq2

libraries were prepared as described previously[19,20] with slight modifications. Briefly, total RNA was captured and purified on RNAClean XP beads (Beckman Coulter, Brea, CA, USA). Polyadenylated mRNA was then selected using an anchored oligo(dT) primer (5′–AAGCAGTGGTATCAACGCAGAGTACT 30VN-3′) and converted to cDNA *via* reverse transcription. First strand cDNA was subjected to limited PCR amplification followed by Tn5 transposon based fragmentation using the Nextera XT DNA Library Preparation Kit (Illumina, San Diego, CA, USA). The samples were then PCR amplified for 18 cycles using barcoded primers such that each sample carries a specific combination of eight base Illumina P5 and P7 barcodes and pooled together prior to Smart sequencing. Smart-seq paired-end sequencing was performed on an Illumina NextSeq500 using 2 × 38 bp reads. Trimmomatic[42] (v0.36) was used to remove Illumina adapters, base pairs lower than 30 Phred quality score, and reads shorter than 20 bases. STAR[43] (v2.7.1a) was used to align reads to the GENCODE GRCm38/mm10 M16 genome primary assembly.[44] Gene level counts were calculated using feature Counts[45] (v1.28.1) in R[46] (v3.4.4). Gene level counts were calculated as variance stabilized transcripts per kilobase (VSTpk). VSTpk expression represents how many transcripts matched to a gene per 1000 base pairs of gene length, with extra normalization to control for differences in the varying sequencing depth per sample. Replicated samples were checked for similarity by Pearson correlation scores (≥ 0.90) on transcripts with higher than an average of 5 reads and below the 99th percentile of reads counted. Heatmap and PCA plots (R packages: heatmap,[47] ggbiplot[48,49] were created from $\log_2$-transformed raw gene counts from feature Counts. Differential gene expression analysis was performed using DESeq2[50] and genes with a $\log_2$-fold-change > 1 or < 1; P-value < 0.05 and a minimum mean read expression count > 30 were determined as DEGs.

Statistical analysis

Statistical analysis was performed using Prism 8 (GraphPad Software, San Diego, CA, USA). Differences between two groups were compared using a non-parametric Mann–Whitney U-test. Differences between three or more groups were calculated using a non-parametric Kruskal-Wallis test. Not significant, not displayed; ($*P < 0.05$; $**P < 0.01$; $***P < 0.001$; $****P < 0.0001$). All figures show the mean ± s.e.m. Differences are not significant unless stated otherwise.

ACKNOWLEDGMENTS

We thank the Hugh Green Cytometry Centre for technical assistance with cell sorting and the Biomedical Research Unit at the Malaghan Institute of Medical Research for animal husbandry to generate the BCL6$^{fl/fl}$.4C13R.CD4^{cre} mouse line. This work was funded by Independent Research Organization funding from the Health Research Council of New Zealand and the Marjorie Barclay Trust. The authors declare no competing financial interests.

AUTHOR CONTRIBUTIONS

Jodie Chandler: Conceptualization; data curation; formal analysis; methodology; visualization; writing – original draft; writing – review and editing. **Melanie Prout:** Data curation; formal analysis. **Sam Old:** Formal analysis; visualization. **Cynthia Morgan:** Formal analysis. **Franca Ronchese:** Conceptualization; investigation; writing – review and editing. **Christophe Benoist:** Methodology; resources. **Graham Le Gros:** Conceptualization; formal analysis; funding acquisition; project administration; supervision; writing – review and editing.

CONFLICT OF INTEREST

We declare that the research was conducted in the absence of any commercial or financial relationships that could be construed as a potential conflict of interest.

DATA AVAILABILITY STATEMENT

The data that support the findings of this study are openly available in Zenodo at http://doi.org/10.5281/zenodo.7048910.

REFERENCES

1. Johnston RJ, Poholek AC, DiToro D. *et al.* Bcl6 and Blimp-1 are reciprocal and antagonistic regulators of T follicular helper cell differentiation. *Science* 2009; **325**: 1006–1010.
2. Yu D, Rao S, Tsai LM. *et al.* The transcriptional repressor Bcl-6 directs T follicular helper cell lineage commitment. *Immunity* 2009; **31**: 457–468.
3. Breitfeld D, Ohl L, Kremmer E. *et al.* Follicular B helper T cells express CXC chemokine receptor 5, localize to B cell follicles, and support immunoglobulin production. *J Exp Med* 2000; **192**: 1545–1552.
4. Schaerli P, Willimann K, Lang AB. *et al.* CXC chemokine receptor 5 expression defines follicular homing T cells with B cell helper function. *J Exp Med* 2000; **192**: 1553–1562.
5. Reinhardt RL, Liang HE, Locksley RM. Cytokine-secreting follicular T cells shape the antibody repertoire. *Nat Immunol* 2009; **10**: 385–393.
6. King IL, Mohrs M. IL-4-producing CD4$^+$ T cells in reactive lymph nodes during helminth infection are T follicular helper cells. *J Exp Med* 2009; **206**: 1001–1007.
7. Glatman Zaretsky A, Taylor JJ, King IL, Marshall FA, Mohrs M, Pearce EJ. T follicular helper cells differentiate from Th2 cells in response to helminth antigens. *J Exp Med* 2009; **206**: 991–999.
8. Crotty S. Follicular helper CD4 T cells (TFH). *Annu Rev Immunol* 2011; **29**: 621–663.
9. Ballesteros-Tato A, Randall TD, Lund FE, Spolski R, Leonard WJ, Leon B. T follicular helper cell plasticity shapes pathogenic T helper 2 cell-mediated immunity to inhaled house dust mite. *Immunity* 2016; **44**: 259–273.

10. Coquet JM, Schuijs MJ, Smyth MJ. *et al*. Interleukin-21-producing CD4$^+$ T cells promote type 2 immunity to house dust mites. *Immunity* 2015; **43**: 318–330.
11. Hondowicz BD, An D, Schenkel JM. *et al*. Interleukin-2-dependent allergen-specific tissue-resident memory cells drive asthma. *Immunity* 2016; **44**: 155–166.
12. Pyle CJ, Labeur-Iurman L, Groves HT. *et al*. Enhanced IL-2 in early life limits the development of TFH and protective antiviral immunity. *J Exp Med* 2021; **218**: e20201555.
13. Yusuf I, Kageyama R, Monticelli L. *et al*. Germinal center T follicular helper cell IL-4 production is dependent on signaling lymphocytic activation molecule receptor (CD150). *J Immunol* 2010; **185**: 190–202.
14. Prout MS, Kyle RL, Ronchese F, Le Gros G. IL-4 is a key requirement for IL-4 and IL-4/IL-13 expressing CD4 Th2 subsets in lung and skin. *Front Immunol* 2018; **9**: 1211.
15. Roediger B, Kyle R, Yip KH. *et al*. Cutaneous immunosurveillance and regulation of inflammation by group 2 innate lymphoid cells. *Nat Immunol* 2013; **14**: 564–573.
16. Camberis M, Prout M, Tang SC. *et al*. Evaluating the *in vivo* Th2 priming potential among common allergens. *J Immunol Methods* 2013; **394**: 62–72.
17. Gowthaman U, Chen JS, Zhang B. *et al*. Identification of a T follicular helper cell subset that drives anaphylactic IgE. *Science* 2019; **365**: 883.
18. Clement RL, Daccache J, Mohammed MT. *et al*. Follicular regulatory T cells control humoral and allergic immunity by restraining early B cell responses. *Nat Immunol* 2019; **20**: 1360–1371.
19. Picelli S, Bjorklund AK, Faridani OR, Sagasser S, Winberg G, Sandberg R. Smart-seq2 for sensitive full-length transcriptome profiling in single cells. *Nat Methods* 2013; **10**: 1096–1098.
20. Picelli S, Faridani OR, Bjorklund AK, Winberg G, Sagasser S, Sandberg R. Full-length RNA-seq from single cells using smart-seq2. *Nat Protoc* 2014; **9**: 171–181.
21. Tibbitt CA, Stark JM, Martens L. *et al*. Single-cell RNA sequencing of the T helper cell response to house dust mites defines a distinct gene expression signature in airway Th2 cells. *Immunity* 2019; **51**: 169–184.
22. Morimoto Y, Hirahara K, Kiuchi M. *et al*. Amphiregulin-producing pathogenic memory T helper 2 cells instruct eosinophils to secrete osteopontin and facilitate airway fibrosis. *Immunity* 2018; **49**: 134–150.
23. Wambre E, Bajzik V, DeLong JH. *et al*. A phenotypically and functionally distinct human TH2 cell subpopulation is associated with allergic disorders. *Sci Transl Med* 2017; **9**: eaam9171.
24. Wang X, Li Z, Naganuma A, Ye BH. Negative autoregulation of BCL-6 is bypassed by genetic alterations in diffuse large B cell lymphomas. *Proc Natl Acad Sci USA* 2002; **99**: 15018–15023.
25. Hollister K, Kusam S, Wu H. *et al*. Insights into the role of Bcl6 in follicular Th cells using a new conditional mutant mouse model. *J Immunol* 2013; **191**: 3705–3711.
26. Tai PC, Sun L, Spry CJ. Effects of IL-5, granulocyte/macrophage colony-stimulating factor (GM-CSF) and IL-3 on the survival of human blood eosinophils *in vitro*. *Clin Exp Immunol* 1991; **85**: 312–316.
27. Shen T, Kim S, Do JS. *et al*. T cell-derived IL-3 plays key role in parasite infection-induced basophil production but is dispensable for *in vivo* basophil survival. *Int Immunol* 2008; **20**: 1201–1209.
28. Johansson MW. Activation states of blood eosinophils in asthma. *Clin Exp Allergy* 2014; **44**: 482–498.
29. MacGlashan D Jr. Marked differences in the signaling requirements for expression of CD203c and CD11b versus CD63 expression and histamine release in human basophils. *Int Arch Allergy Immunol* 2012; **159**: 243–252.
30. Wan YY. GATA3: a master of many trades in immune regulation. *Trends Immunol* 2014; **35**: 233–242.
31. Wang Y, Su MA, Wan YY. An essential role of the transcription factor GATA-3 for the function of regulatory T cells. *Immunity* 2011; **35**: 337–348.
32. Sawant DV, Sehra S, Nguyen ET. *et al*. Bcl6 controls the Th2 inflammatory activity of regulatory T cells by repressing Gata3 function. *J Immunol* 2012; **189**: 4759–4769.
33. Sawant DV, Wu H, Yao W, Sehra S, Kaplan MH, Dent AL. The transcriptional repressor Bcl6 controls the stability of regulatory T cells by intrinsic and extrinsic pathways. *Immunology* 2015; **145**: 11–23.
34. Harvie M, Camberis M, Tang SC, Delahunt B, Paul W, Le Gros G. The lung is an important site for priming CD4 T-cell-mediated protective immunity against gastrointestinal helminth parasites. *Infect Immun* 2010; **78**: 3753–3762.
35. van Panhuys N, Tang SC, Prout M. *et al*. *In vivo* studies fail to reveal a role for IL-4 or STAT6 signaling in Th2 lymphocyte differentiation. *Proc Natl Acad Sci USA* 2008; **105**: 12423–12428.
36. Lonnberg T, Svensson V, James KR. *et al*. Single-cell RNA-seq and computational analysis using temporal mixture modelling resolves Th1/Tfh fate bifurcation in malaria. *Sci Immunol* 2017; **2**: eaal2192.
37. Tsukumo S, Unno M, Muto A. *et al*. Bach2 maintains T cells in a naive state by suppressing effector memory-related genes. *Proc Natl Acad Sci USA* 2013; **110**: 10735–10740.
38. Ochiai K, Katoh Y, Ikura T. *et al*. Plasmacytic transcription factor Blimp-1 is repressed by Bach2 in B cells. *J Biol Chem* 2006; **281**: 38226–38234.
39. Mondal A, Sawant D, Dent AL. Transcriptional repressor BCL6 controls Th17 responses by controlling gene expression in both T cells and macrophages. *J Immunol* 2010; **184**: 4123–4132.
40. Toney LM, Cattoretti G, Graf JA. *et al*. BCL-6 regulates chemokine gene transcription in macrophages. *Nat Immunol* 2000; **1**: 214–220.
41. Zhu J, Yamane H, Paul WE. Differentiation of effector CD4 T cell populations (*). *Annu Rev Immunol* 2010; **28**: 445–489.
42. Bolger AM, Lohse M, Usadel B. Trimmomatic: a flexible trimmer for Illumina sequence data. *Bioinformatics* 2014; **30**: 2114–2120.

43. Dobin A, Davis CA, Schlesinger F. *et al.* STAR: ultrafast universal RNA-seq aligner. *Bioinformatics* 2013; **29**: 15–21.
44. Frankish A, Diekhans M, Ferreira AM. *et al.* GENCODE reference annotation for the human and mouse genomes. *Nucleic Acids Res* 2019; **47**: D766–D773.
45. Liao Y, Smyth GK, Shi W. The R package Rsubread is easier, faster, cheaper and better for alignment and quantification of RNA sequencing reads. *Nucleic Acids Res* 2019; **47**: e47.
46. RCoreTeam. R: A Language and Environment for Statistical Computing. Vienna: R Foundation for Statistical Computing; 2019.
47. Kolde R. pheatmap: Pretty Heatmaps. R package version 1.0.12 ed: R; 2019.
48. Vu VQ. ggbiplot: A ggplot2 based biplot. R package version 0.55 ed: R; 2011.
49. Wickham H. Ggplot2: Elegant Graphics for Data Analysis. New York: Springer; 2009.
50. Love MI, Huber W, Anders S. Moderated estimation of fold change and dispersion for RNA-seq data with DESeq2. *Genome Biol* 2014; **15**: 550.

SUPPORTING INFORMATION

Additional supporting information may be found online in the Supporting Information section at the end of the article.